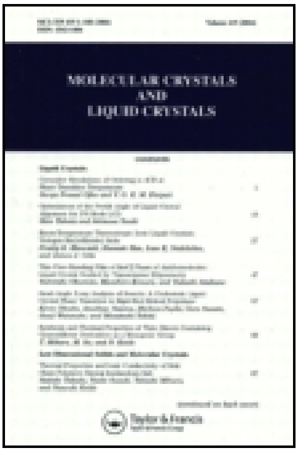

Molecular Crystals and Liquid Crystals
Publication details, including instructions for authors and subscription information:
http://www.tandfonline.com/loi/gmcl20

Supramolecular Liquid Crystals Induced by Hydrogen-Bonding Interactions between Non-Mesomorphic Compounds. II. Effect of Lateral Substitution

Magdi M. Naoum [a], Abdel Gawad. A. Fahmi [a] & Wedad A. Almllal [a]
[a] Department of Chemistry, Faculty of Science, Cairo University, Giza, Egypt

Version of record first published: 18 Mar 2010

To cite this article: Magdi M. Naoum, Abdel Gawad. A. Fahmi & Wedad A. Almllal (2010): Supramolecular Liquid Crystals Induced by Hydrogen-Bonding Interactions between Non-Mesomorphic Compounds. II. Effect of Lateral Substitution, Molecular Crystals and Liquid Crystals, 518:1, 109-128

To link to this article: http://dx.doi.org/10.1080/15421400903568070

Mol. Cryst. Liq. Cryst., Vol. 518: pp. 109–128, 2010
Copyright © Taylor & Francis Group, LLC
ISSN: 1542-1406 print/1563-5287 online
DOI: 10.1080/15421400903568070

Taylor & Francis
Taylor & Francis Group

Supramolecular Liquid Crystals Induced by Hydrogen-Bonding Interactions between Non-Mesomorphic Compounds. II. Effect of Lateral Substitution

MAGDI M. NAOUM, ABDEL GAWAD. A. FAHMI, AND WEDAD A. ALMLLAL

Department of Chemistry, Faculty of Science, Cairo University, Giza, Egypt

Two groups of the laterally methyl-substituted 1:1 associates between 4-(4′-pyridylazo-3-methylphenyl)-4″-substituted benzoates and 4-substituted benzoic acids were prepared to investigate the effect of different substituents, either on the pyridine-based derivatives or on the acid component, on the extent and stability of the supramolecular liquid crystal phases induced by intermolecular hydrogen bonding. In the first series of complexes (Group ***A****), the non-mesomorphic pyridine-based derivative carries, in addition to the lateral methyl group, a terminal polar substituent, whereas the benzoic acid component, which is mesomorphic, carries an alkoxy group of varying chain length. The other series of complexes (Group* ***B****) is composed of the same pyridine-based derivatives, but the benzoic acid carries a small compact polar group. The complexes prepared in both series were characterized for their mesophase behavior by differential scanning calorimetry (DSC), and polarized light microscopy (PLM). Six pyridine-based derivatives, with molecular formula* $4\text{-}X\text{-}C_6H_4COOC_6H_3(3\text{-}CH_3)\text{-}N{=}N\text{-}C_5H_4N$*, were prepared. The substituent, X, varies between* CH_3O*,* CH_3*, H, Cl, Br, and CN. The smectic C mesophase is observed in most of group* ***A*** *complexes, and the nematic phase is the mesophase induced in some of group* ***B*** *complexes.*

Keywords Binary mixtures; 4-(4′-pyridylazo-3-methylphenyl)-4″-substituted benzoates; 4-substituted benzoic acids; supramolecular LCs

Introduction

In previous studies, the effect of a terminal polar substituent and an alkoxy chain of variable length on the mesophase behavior of phenyl benzoate-based materials [1] was investigated. Not all of the derivatives are mesomorphic, whereas the inversion of the ester group, in the same type of compounds, has led to a significant variation of their mesophase behavior. Later on, the introduction of a third benzene ring (within a C_6H_4-N=N- moiety) to the phenyl benzoate molecule [2] yielded compounds that are all mesomorphic and possess high melting (T_m) and clearing

---

Address correspondence to Magdi M. Naoum, Department of Chemistry, Faculty of Science, P.O. 12613, Cairo University, Giza, Egypt. E-mail: magdinaoum@yahoo.co.uk

(***T***$_C$) temperatures, indicating the existence of strong attractive intermolecular forces both in the solid phase and in the mesophase. Generally, lateral substitution decreases the thermal stability of both solid and meso phases [3–8]; this is frequently used in lowering the melting temperatures to match industrial application requirements. On the other hand, the role of hydrogen bonding in molecular recognition and self-assembly of liquid-crystalline phases has been investigated in recent years and significant work has been conducted [9,10]. A single hydrogen bond between the carboxyl and pyridine moieties was found [10,11] to be extremely fruitful in the formation of liquid crystals. Complementary components may be either mesomorphic or non-mesomorphic; in either case, however, novel liquid crystals can be obtained. Although in many cases [11] none of the two complementary components bears an alkyl or alkoxy chain, most of the complexes examined proved to exhibit nematic mesomorphism with high clearing temperatures. In such case, the nature of the terminal substituents on either side of the supramolecular complex was found to have crucial effect upon mesomorphism. These results have encouraged us to widen our previous study [12–14] to test the effect of lateral substitution on the possibility of mesophase formation and, consequently, on the stability of the complexes formed between the non-mesomorphic 4-(4′-pyridylazo-3-methylphenyl)-4″-substituted benzoates (**I**$_{a-f}$) and each of the five mesomorphic 4-alkoxybenzoic acids (**II***8*–**II***16*) and the seven non-mesomorphic 4-substituted benzoic acids (**II**$_{a-g}$).

The present study represents a trial to reduce the melting point of the previously [12] investigated supramolecular complexes by introducing a lateral methyl group into position 3 of the central benzene ring of the previously investigated pyridine-based component, **III**. The methyl group was chosen on the basis of its mild polarity; in addition, it is bulky enough to modify the molecular arrangement in both the crystal lattice and in the mesophase.

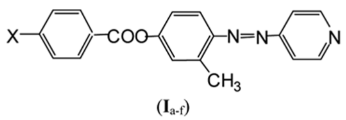

(**I**$_{a\text{-}f}$)

I$_a$, X=CH_3O, **I**$_b$, X=CH_3, **I**$_c$, X=H, **I**$_d$, X= Cl, **I**$_e$, X= Br, **I**$_f$, X=CN

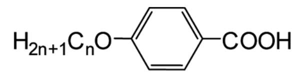

(**II***8* – **II***16*)

II*8*, n = 8, **II***10*, n = 10, **II***12*, n = 12, **II***14, n = 14* and **II***16*, n = 16.

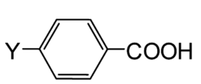

(**II**$_{a\text{-}g}$)

II$_a$, Y=CH_3O, **II**$_b$, Y=CH_3, **II**$_c$, Y=H, **II**$_d$, Y= Cl, **II**$_e$, Y=Br, **II**$_f$, Y= CN, **II**$_g$, Y= NO_2

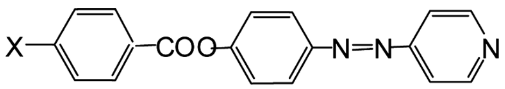

(**III**$_{a\text{-}e}$)

III$_a$, Y=CH_3O, **III**$_b$, Y=CH_3, **III**$_c$, Y=H, **III**$_d$, Y=Br, **II**$_e$, Y= NO_2

Experimental

Chemicals were of very pure grades and purchased from the following companies: Fluka (Buchs, Switzerland), Aldrich (Milwaukee, Wisconsin), and E. Merck (Darmstadt, Germany).

Preparation of Materials

The pyridine-based azo dyes (**I**$_{a-f}$) were prepared according to the following scheme:

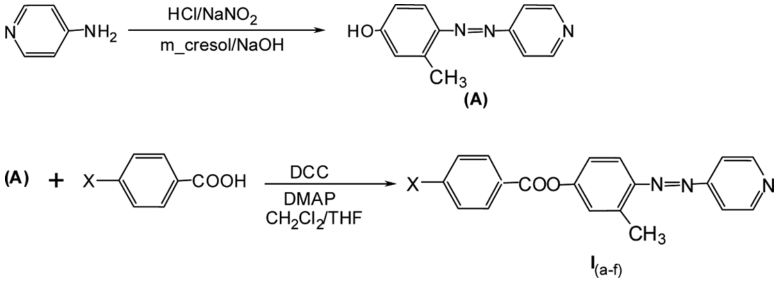

Preparation of 4-(4′-pyridylazo)-3-methylphenol (A). This was prepared according to the method described by Song *et al.* [15] from 4-aminopyridine and m-cresol. The yield of the crude product was 65% that melts at 232.6°C.

Preparation of 4-(4′-pyridylazo-3-methylphenyl)-4″-substituted benzoates (I$_{a-f}$). This was prepared from the azo **A** and its molar equivalent of the acid (**II**) according to the method described before [12]. The solids (≈50% yield) obtained, after being twice crystallized from ethanol, the purity was checked by TLC and found to be pure and possess sharp melting temperatures as measured by DSC and are given in Table 1. Elemental analyses were conducted for these newly prepared compounds and the results are included in Table 1.

Physical Characterization

Calorimetric measurements were carried out using a PL-DSC of Polymer Laboratories, Leicestershire, England. The instrument was calibrated for temperature, heat, and heat flow according to the method recommended by Cammenga *et al.* [16].

Transition temperatures were checked and types of mesophases identified for adducts prepared with a standard polarized light microscope (PLM, Wild, Heerberugg, Germany) attached to a home made hot stage.

Table 1. Melting points (°C), melting enthalpies (kJ/mol), and elemental analyses of the pyridine-based azo dyes, **I**$_{a-f}$

Comp. number	X	T_m	ΔH_m	Elemental analyses found (calc.) % C	% H	% N
I$_a$	CH_3O	154.1	39.3	68.78 (69.15)	5.19 (4.93)	12.04 (12.10)
I$_b$	CH_3	118.3	23.2	72.46 (72.40)	5.25 (5.17)	12.80 (12.68)
I$_c$	H	109.7	21.9	71.75 (71.91)	5.07 (4.76)	13.03 (13.24)
I$_d$	Cl	162.4	29.8	65.11 (64.87)	4.19 (4.01)	11.78 (11.95)
I$_e$	Br	176.9	37.6	59.98 (57.59)	3.70 (3.56)	10.49 (10.61)
I$_f$	CN	179.3	28.3	69.87 (70.17)	4.33 (4.18)	16.25 (16.37)

For the investigation of the supramolecular complexes (**I**/**II**), binary mixtures of any two complementary components were prepared in a 1:1 molar ratio by melting the appropriate amounts of each component, stirring to give an intimate blend, and then cooling with stirring to room temperature.

For the construction of binary phase diagrams, the mixtures were prepared to cover the whole range of composition. In the phase diagrams, constructed by plotting transition temperatures *versus* mixture composition, the symbol "○" denotes solid-mesophase, "□" mesophase-isotropic transitions, "•" mesophase another mesophase, and "Δ" eutectic temperature, the temperature at which the solid mixture starts to melt.

Results and Discussion

Confirmation of Molecular Structure

The molecular structures of the newly prepared pyridine-based derivatives ($\mathbf{I}_{a-f}$) were confirmed via elemental analyses, infrared (IR), nuclear magnetic resonance (NMR), and mass spectra. The results were in agreement, within permissible limits, with the proposed structures.

Phase Behavior

As can be seen from Table 1, all of the derivatives prepared are of high melting points, and none is mesomorphic. In order to investigate the effect of introducing the lateral methyl group into the central benzene ring on the phase behavior of compounds of the type **I**, comparison was made with the corresponding values, previously reported [12] for 4-(4′-pyridylazophenyl)-4″-substituted benzoates ($\mathbf{III}_{a-e}$). The data of the correspondingly substituted derivatives from series **I** and **III** revealed that the introduction of a lateral methyl group into the central benzene ring resulted in a sound lowering of the melting point. These preliminary results have encouraged us to extend our investigation to constitute all possible supramolecular hydrogen-bonded complexes formed between the prepared, laterally substituted, pyridine-based derivatives, $\mathbf{I}_{a-f}$, and two series of 4-substituted benzoic acids. The first group of acids tested is the mesomorphic homologues of 4-alkoxy benzoic acids, **II***n*, in which *n* varies between 8 and 16 carbons. In the second series of acids, $\mathbf{II}_{a-g}$, all are non-mesomorphic and each is 4-substituted with a small compact polar group (Y) that is changed between CH_3O, CH_3, H, Cl, Br, CN, and NO_2.

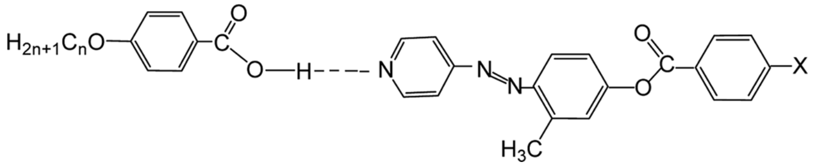

Group A

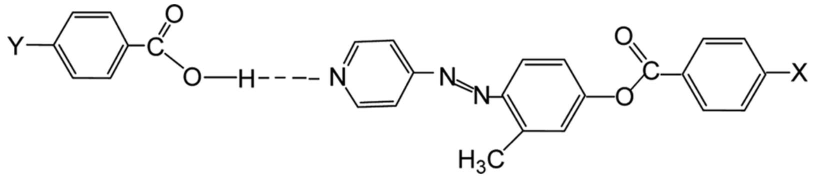

Group B

Independent of the substituent Y, none of the derivatives of the acids, $\mathbf{II}_{a-g}$, is mesomorphic, whereas all the 4-alkoxybenzoic acids are mesomorphic. The lower homologues, **II***8*–**II***12*, are polymorphic, possessing both nematic (N) and smectic C (SmC) mesophases, whereas the higher homologues, **II***14* and **II***16*, are purely smectogenic, possessing the SmC phase as the only mesophase. Such a difference in behavior of the acids would definitely affect the mesophase behavior of their complexes with the non-mesomorphic pyridine-based component in variable manners.

Group A Supramolecular Complexes. In order to confirm the formation of a supramolecular complex, the binary phase diagrams for each of the pyridine-based components, $\mathbf{I}_{a-f}$, with two selected homologues of the acids **II***n* were constructed, and the resulting binary phase behavior was investigated The binary phase diagrams obtained are represented graphically in Figs. 1–6. Generally, the strength of the hydrogen bond, leading to the supramolecular liquid crystals, will affect, in one way or another, the phase behavior of the resulting complex [17]. In this pyridine/acid binary system, the association is primarily affected by the basicity of the pyridine-based component (**I**), as well as the acidity of the proton-donor, the acid (**II**).

Binary Phase Behavior.

Binary mixtures of the electron-donating (CH_3O or CH_3) substituted derivatives (I_a and I_b) with 4-alkoxybenzoic acids. Expectedly, the introduction of an electron-donating group, in a para position within the base **I**, may, through inductive and/or mesomeric effects, increase slightly the electron density on the pyridine nitrogen and, consequently, increases to some extent the basicity of the base component ($\mathbf{I}_a$ or $\mathbf{I}_b$), of the hydrogen-bonded complex. Figure 1 represents the binary phase diagrams constructed for the two binary systems prepared from the methoxy-substituted pyridine-based derivative ($\mathbf{I}_a$) with two homologues of the acids, **II***12*

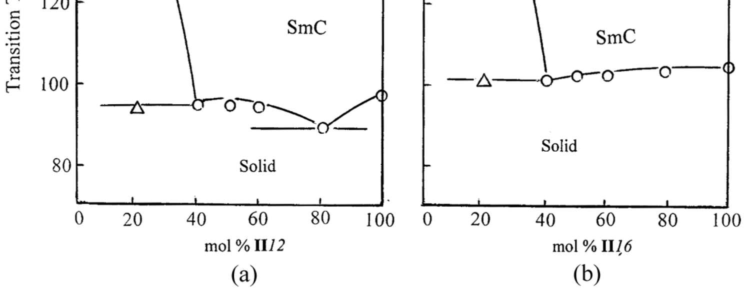

Figure 1. Binary phase diagram of the methoxy-substituted pyridine-based derivative ($\mathbf{I}_a$) with (a) dodecyloxy benzoic acid and (b) hexadecyloxy benzoic acid.

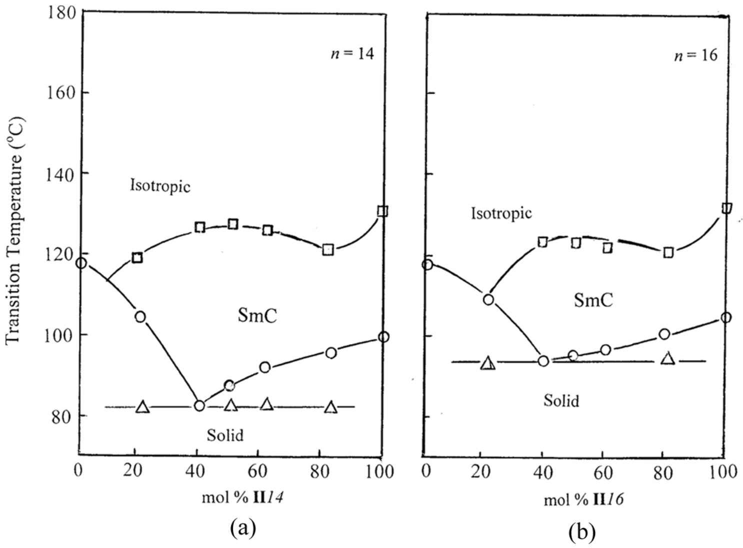

Figure 2. Binary phase diagram of the methyl-substituted pyridine-based derivative (I_b) with (a) tetradecyloxy benzoic acid and (b) hexadecyloxy benzoic acid.

and **II***16*, taken as examples, respectively. As can be seen from the figure, both homologues of the acids retain the SmC phase within the intermediate range of composition. The nematic phase of the lower acid is widened by the addition of the non-mesomorphic component, I_a, whereas with the higher smectogenic acid homologue, **II***16*, the nematic phase is induced upon the first addition of the base, I_a. The formation of liquid-crystalline complexes through hydrogen bonding in the

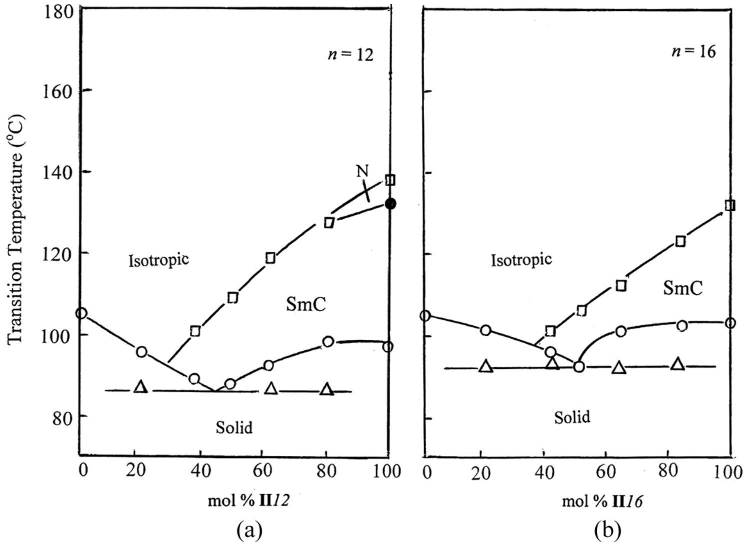

Figure 3. Binary phase diagram of the unsubstituted pyridine-based derivative (I_c) with (a) dodecyloxy benzoic acid and (b) hexadecyloxy benzoic acid.

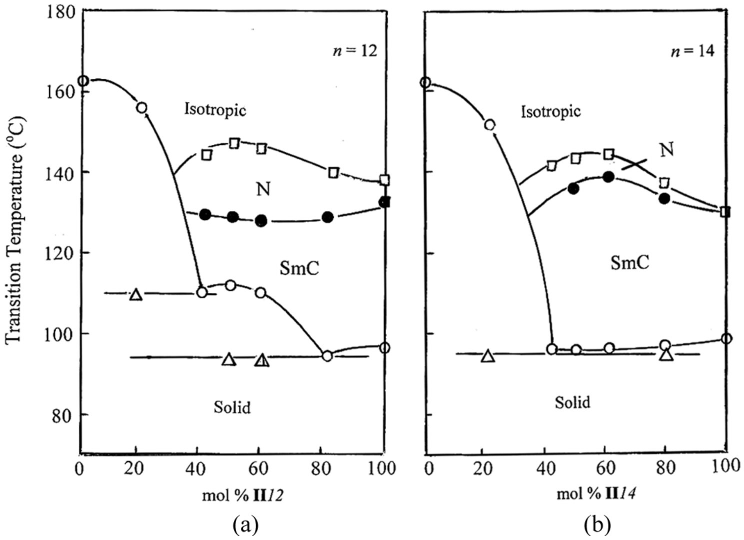

Figure 4. Binary phase diagram of the chloro-substituted pyridine-based derivative ($\mathbf{I_d}$) with (a) dodecyloxy benzoic acid and (b) tetradecyloxy benzoic acid.

1:1 complex is evidenced in both systems by the pronounced enhancement of the nematic stability, $T_{\text{N-I}} = 154.4°\text{C}$ and 145.7°C, in both systems, respectively. A further observation can be deduced from Fig. 1; that is, a solid complex is formed with the lower acid homologue as evidenced by the two eutectic temperatures one preceding and the other following the 1:1 composition.

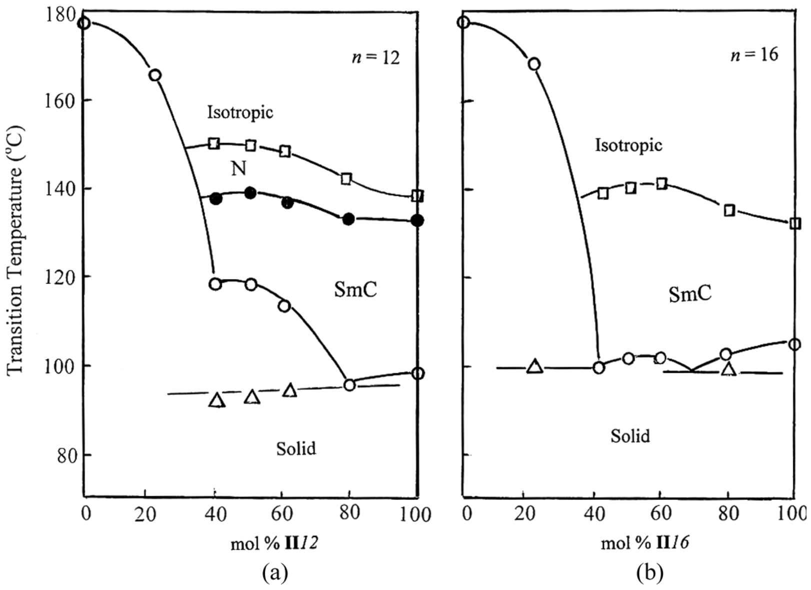

Figure 5. Binary phase diagram of the bromo-substituted pyridine-based derivative ($\mathbf{I_e}$) with (a) dodecyloxy benzoic acid and (b) hexadecyloxy benzoic acid.

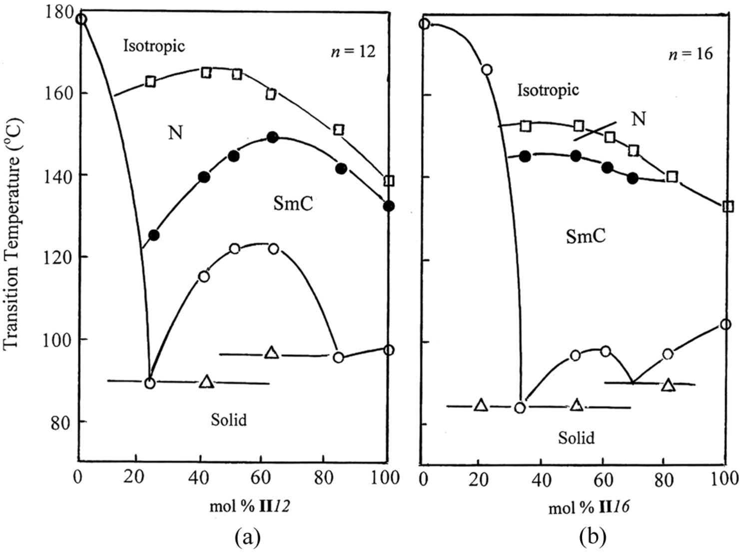

Figure 6. Binary phase diagram of the cyano-substituted pyridine-based derivative ($\mathbf{I}_f$) with (a) dodecyloxy benzoic acid and (b) hexadecyloxy benzoic acid.

Similar investigation of the phase behavior of the methyl-substituted analogue ($\mathbf{I}_b$) with two representative homologues of the acid (**II***14* and **II***16*), as given in Fig. 2, revealed that supramolecular complexes are again formed between the proton donors, the acids, and the relatively still strong proton-acceptor, the base $\mathbf{I}_b$. Complex formation is again evidenced from the enhancement of the SmC mesophase stability of the 1:1 complexes.

Binary mixtures of the unsubstituted derivative (I_c) with 4-alkoxybenzoic acids. Examining the binary phase behavior of the unsubstituted analogue of the proton acceptors, $\mathbf{I}_c$, again with two representative acid homologues (**II***12* and **II***16*), as given in Fig. 3, revealed that the addition of the non-mesomorphic component, $\mathbf{I}_c$, gradually destroys the SmC mesophase of the acid up to the addition of more than 60 mol% of $\mathbf{I}_c$. That is, the 1:1 molar composition is still exhibiting an SmC mesophase. Comparing these results with those of the correspondingly laterally substituted analogue [12], which still exhibits the SmC mesophase and showed evidence for the 1:1 complex, revealed that the introduction of a lateral methyl group into the central benzene ring greatly disturbs its mesophase behavior.

Binary mixtures of the electron-withdrawing (Cl, Br, and CN) substituted derivatives (I_{d-f}) with 4-alkoxybenzoic acids. As expected, these three electron-withdrawing substituents on the proton-acceptor complementary components interact electronically with the rest of the molecule, in different manners, hence imparting an electron-density to the pyridine-nitrogen to different extents. Thus, whereas the cyano group in $\mathbf{I}_f$ induces an electronic shift toward itself, the halogen substituents, Cl or Br, interact electronically with the rest of the molecule in two opposing manners. That is, due to their high electronegativity, they attract electrons by inductive effect, whereas by their mesomeric effect their lone pairs of electrons are directed toward the pyridine nitrogen. These two opposing effects may render the basicity of the molecule of $\mathbf{I}_d$ or $\mathbf{I}_e$ more or less comparable with the unsubstituted analogue, $\mathbf{I}_c$. Examining the binary phase diagrams of the chloro- or bromo-substituted pyridine-based derivatives with representative homologues of the acid, as given in Figs. 4 and 5, respectively, revealed that the basicity of $\mathbf{I}_d$ and $\mathbf{I}_e$ are still adequate to form the supramolecular hydrogen-bonded complexes at the 1:1 molar composition. This is evident from the figures that show enhanced T_C-composition dependences.

It is clear from Fig. 4 that the chloro-substituted derivative forms solid complexes with **II***12* as evidenced by the two eutectic points before and after the 1:1 molar ratio. Complexes are also observed in the mesophases as evidenced by the enhanced stability of the N mesophase (*i.e.*, $T_{N\text{-}I}$). Similar behavior is also observed for the other acid homologue in the system $\mathbf{I}_d$/**II***14*, where enhancement was observed in both the SmC and the N mesophases.

With respect to the bromo-substituted derivative, solid complexes are formed between $\mathbf{I}_e$ and either of the two acid homologues, **II***12* and **II***16*, as can be seen from Fig. 5. Complex formation is also observed in the mesophases. Thus, mixtures with the lower acid homologue, **II***12*, show enhanced SmC and N phase stability. The other system with the higher acid homologue, **II***16*, does not exhibit the N mesophase. When compared with the unsubstituted analogue, $\mathbf{I}_c$, it is clear that substitution with a halogen atoms furnishes complexes with higher stabilities, indicating that the electron-donating effect for both halogen atoms with the remainder of the molecules overcomes their electron-withdrawing inductive effect, thus rendering the molecule more basic compared with the unsubstituted analogue. Accordingly, their hydrogen-bonded complexes with the acids are more stable. Also, observe in Fig. 5 that solid complexes are formed in both systems as evidenced by the two eutectic temperatures. On the other hand, comparison of our present data with those reported previously [12] for the laterally-neet 4-bromo analogue that showed complex formation independent of the alkoxy-chain length in both the solid and mesophase revealed that lateral substitution by a methyl group into the central benzene ring resulted, again, in a decrease in the melting point as well as in the stability of the mesophase.

The results of the cyano-substituted analogue, $\mathbf{I}_f$, with either of the two acid homologues, **II***12* and **II***16* are surprising. Usually, the cyano group with its strong electron-withdrawing character is expected to diminish the electron density on the pyridine nitrogen as well as its basicity and proton-acceptor capability; consequently, the possibility of hydrogen-bonded complex formation is expectedly reduced. Practically, the reverse holds true. As can be seen from Fig. 6, which reproduces the binary phase diagrams of the pyridine-based component, $\mathbf{I}_f$, with the two acid homologues, **II***12* and **II***16*, complex formation is strongly effected in both the solid and the mesophase. This may be attributed, as concluded before [12], to the possible anti-parallel alignment of such strong dipolar molecules so that it enhances mesophase stability. Comparing the present data with those reported for the laterally-neet 4-nitro analogue [12], which showed no solid complex formation, revealed that lateral methyl substitution, in the cyano analog $\mathbf{I}_f$, forces the rod-like molecules apart, thus reducing the strong dipolar repulsive forces and, at the same time, allow smooth anti-parallel alignment of molecules, either in the solid or in the mesophase. This is clear from Fig. 6, where solid complexes were observed, as evidenced by the two eutectic points following and preceding the 1:1 molar compositions, as well as the enhancement in the stability of the N and SmC mesophases.

Effect of Alkoxy-Chain Length on Complex Formation. To investigate the effect of alkoxy-chain length on the mesophase behavior of complexes of group **A**, all possible complexes were prepared and similarly characterized. Table 2 and Fig. 7 illustrate the dependences on the acid alkoxy-chain length (*n*) of transition temperatures of the supramolecular complexes (group **A**) prepared from the pyridine-based derivatives and each of the acid homologues. As can be seen from Fig. 7, polar substituents whether electron-donating or electron-withdrawing, on the pyridine-based component, except for $\mathbf{I}_b$ and $\mathbf{I}_c$, are effective in promoting the N mesophase. That is, substituted pyridine-based derivatives with all acid homologues are found to exhibit considerable N temperature range, which decreases with increase of the acid alkoxy-chain length (*n*). Independent of the

Table 2. Phase transition temperatures (°C) of the 1:1 supramolecular hydrogen-bonded complexes[a] of the systems $\mathbf{I}_{a-f}/\mathbf{II}n$ (Group **A**)

System	X	n	$T_{Cr\text{-}C}$	$T_{C\text{-}N}$	$T_{C\text{-}I}$	$T_{N\text{-}I}$
$\mathbf{I}_a/\mathbf{II}8$	CH_3O	8	95.3	120.4	—	153.7
$\mathbf{I}_a/\mathbf{II}10$		10	108.2	121.6	—	156.3
$\mathbf{I}_a/\mathbf{II}12$		12	93.4	125.9	—	154.4
$\mathbf{I}_a/\mathbf{II}14$		14	96.9	122.9	—	147.2
$\mathbf{I}_a/\mathbf{II}16$		16	101.6	129.4	—	145.7
$\mathbf{I}_b/\mathbf{II}8$	CH_3	8	103.5	—	134.8	—
$\mathbf{I}_b/\mathbf{II}10$		10	87.6	—	131.7	—
$\mathbf{I}_b/\mathbf{II}12$		12	89.5	—	129.7	—
$\mathbf{I}_b/\mathbf{II}14$		14	82.1	—	127.2	—
$\mathbf{I}_b/\mathbf{II}16$		16	94.2	—	123.2	—
$\mathbf{I}_c/\mathbf{II}8$	H	8	98.2	—	124.2	—
$\mathbf{I}_c/\mathbf{II}10$		10	82.6	—	106.9	—
$\mathbf{I}_c/\mathbf{II}12$		12	88.0	—	108.3	—
$\mathbf{I}_c/\mathbf{II}14$		14	91.6	—	110.3	—
$\mathbf{I}_c/\mathbf{II}16$		16	92.5	—	127.0	—
$\mathbf{I}_d/\mathbf{II}8$	Cl	8	102.2	128.7	—	155.4
$\mathbf{I}_d/\mathbf{II}10$		10	87.7	128.0	—	150.7
$\mathbf{I}_d/\mathbf{II}12$		12	111.1	128.8	—	146.8
$\mathbf{I}_d/\mathbf{II}14$		14	96.6	136.2	—	143.8
$\mathbf{I}_d/\mathbf{II}16$		16	99.9	—	138.0	—
$\mathbf{I}_d/\mathbf{II}8$	Br	8	92.9	112.2	—	158.4
$\mathbf{I}_e/\mathbf{II}10$		10	88.4	127.2	—	151.8
$\mathbf{I}_e/\mathbf{II}12$		12	118.5	137.8	—	148.0
$\mathbf{I}_e/\mathbf{II}14$		14	97.9	140.0	—	146.0
$\mathbf{I}_e/\mathbf{II}16$		16	101.6	139.5	—	144.0
$\mathbf{I}_f/\mathbf{II}8$	CN	8	110.6	139.5	—	172.9
$\mathbf{I}_f/\mathbf{II}10$		10	88.9	144.0	—	165.4
$\mathbf{I}_f/\mathbf{II}12$		12	122.1	144.5	—	163.9
$\mathbf{I}_f/\mathbf{II}14$		14	94.2	147.1	—	159.5
$\mathbf{I}_f/\mathbf{II}16$		16	97.2	146.5	—	153.4

[a] Values given are for the 50 mol% compositions.

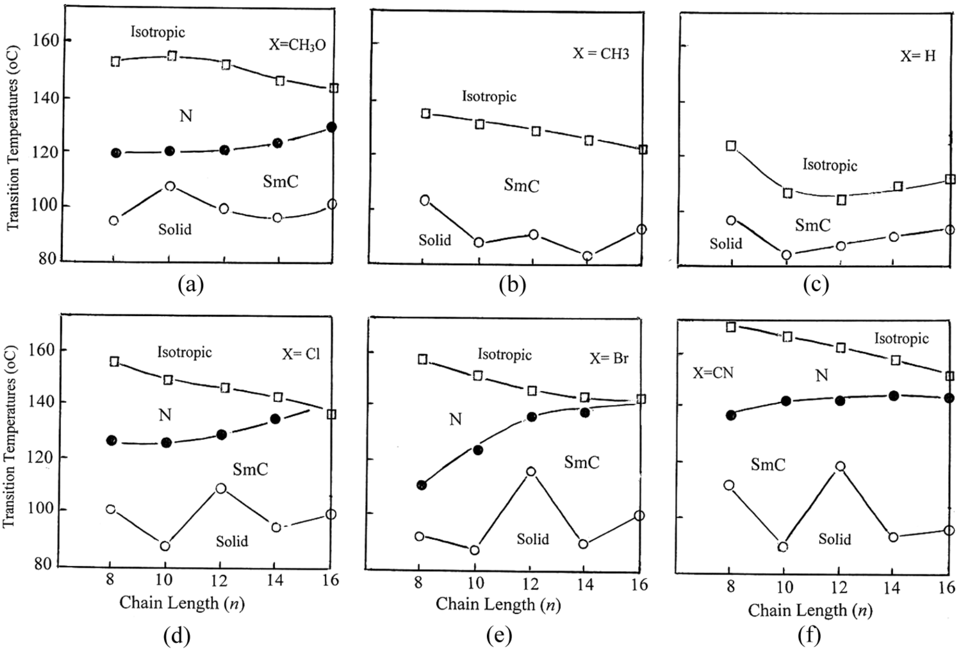

Figure 7. Effect of the alkoxy-chain length (*n*) on the mesophase behavior of the 1:1 complexes of group **A**.

substituent, X, the melting point of the solid complexes is found to be irregularly changing with the chain length (*n*). The stability of the SmC mesophase, $T_{C\text{-}N}$, increases with *n*. The unsubstituted and the methyl-substituted derivatives, $\mathbf{I}_b$ and $\mathbf{I}_c$, behave differently, where they show no N mesophase, whereas the stability of the SmC phase decreases (for $\mathbf{I}_b$) first up to $n = 12$ and then increases again slightly for $n = 14$ and 16 carbons. Except for $\mathbf{I}_b$ and $\mathbf{I}_c$, which are purely smectogenic, the nematic phase is found to decrease upon the increase of *n*.

*Group **B** Supramolecular Complexes.* In this series, of supramolecular liquid crystal complexes, the same proton-acceptors, *i.e.*, the pyridyl azo derivatives, $\mathbf{I}_{a-f}$, were used, this time with the non-mesomorphic benzoic acids, $\mathbf{II}_{a-g}$, 4-substituted with small compact polar group, Y. In the present series (group **B**) of complexes, the two non-mesomorphic components were allowed to interact in the melt leading to the formation of supramolecular liquid crystal complexes. All possible 1:1 molar mixtures, made from each of the six pyridine-based derivatives ($\mathbf{I}_{a-f}$), alternatively, with each of the seven substituted benzoic acids ($\mathbf{II}_{a-g}$), were investigated for their mesophase behavior by DSC and PLM, and the results are collected in Table 3. As can be seen from the table, electron-donating (CH_3O and CH_3), as well as the strong electron-withdrawing (CN), groups induce the nematic phase in the resultant complexes, independent of the type of substituent on the acid complement. Conversely, the unsubstituted derivative, $\mathbf{I}_c$, furnishes complexes that are non-mesomorphic, independent also of the acid used. The halogen-substituted bases, $\mathbf{I}_d$ and $\mathbf{I}_e$, form complexes that are intermediate in behavior. That is, they

Table 3. Phase transition temperatures (°C) of the 1:1 supramolecular hydrogen-bonded complexes[a] of the systems $\mathbf{I}_{a-f}/\mathbf{II}_{a-g}$ (Group **B**)

System	X	Y	$T_{\text{C-N}}$ (T_m)	ΔH_m	$T_{\text{N-I}}$ (T_C)	$\sqrt{T_C}$ ($K^{1/2}$)
$\mathbf{I}_a/\mathbf{II}_a$	CH_3O	CH_3O	131.3	36.6	188.7	21.5
$\mathbf{I}_a/\mathbf{II}_b$		CH_3	133.9	51.7	159.0	20.8
$\mathbf{I}_a/\mathbf{II}_c$		H	107.4	24.4	153.5	20.6
$\mathbf{I}_a/\mathbf{II}_d$		Cl	138.7	44.2	172.1	21.1
$\mathbf{I}_a/\mathbf{II}_e$		Br	134.0	39.2	173.7	21.2
$\mathbf{I}_a/\mathbf{II}_f$		CN	170.9	24.2	197.3	21.7
$\mathbf{I}_a/\mathbf{II}_g$		NO_2	185.7	32.5	213.9	22.1
$\mathbf{I}_b/\mathbf{II}_a$	CH_3	CH_3O	121.7	29.3	163.7	20.9
$\mathbf{I}_b/\mathbf{II}_b$		CH_3	108.0	30.5	114.9	19.7
$\mathbf{I}_b/\mathbf{II}_c$		H	99.0	25.8	111.1	19.6
$\mathbf{I}_b/\mathbf{II}_d$		Cl	108.4	6.2	143.5	20.4
$\mathbf{I}_b/\mathbf{II}_e$		Br	109.6	8.6	147.7	20.5
$\mathbf{I}_b/\mathbf{II}_f$		CN	169.2	29.4	174.2	21.2
$\mathbf{I}_b/\mathbf{II}_g$		NO_2	160.6	24.4	184.9	21.4
$\mathbf{I}_c/\mathbf{II}_a$	H	CH_3O	111.9[b]	22.4	—	—
$\mathbf{I}_c/\mathbf{II}_b$		CH_3	99.0[b]	10.1	—	—
$\mathbf{I}_c/\mathbf{II}_c$		H	102.1[b]	17.1	—	—
$\mathbf{I}_c/\mathbf{II}_d$		Cl	104.1[b]	11.3	—	—
$\mathbf{I}_c/\mathbf{II}_e$		Br	138.0[b]	27.0	—	—
$\mathbf{I}_c/\mathbf{II}_f$		CN	162.5[b]	33.2	—	—
$\mathbf{I}_c/\mathbf{II}_g$		NO_2	168.4[b]	17.4	—	—
$\mathbf{I}_d/\mathbf{II}_a$	Cl	CH_3O	138.3	36.4	191.3	21.5
$\mathbf{I}_d/\mathbf{II}_b$		CH_3	137.6	15.8	151.2	20.6
$\mathbf{I}_d/\mathbf{II}_c$		H	164.4[b]	41.3	—	—
$\mathbf{I}_d/\mathbf{II}_d$		Cl	157.8[b]	44.1	—	—
$\mathbf{I}_d/\mathbf{II}_e$		Br	154.8[b]	21.8	—	—
$\mathbf{I}_d/\mathbf{II}_f$		CN	157.5	15.6	189.1	21.5
$\mathbf{I}_d/\mathbf{II}_g$		NO_2	155.5	12.7	182.5	21.3
$\mathbf{I}_e/\mathbf{II}_a$	Br	CH_3O	136.1	18.6	197.8	21.8
$\mathbf{I}_e/\mathbf{II}_b$		CH_3	146.4	14.1	172.1	21.1
$\mathbf{I}_e/\mathbf{II}_c$		H	177.0[b]	20.3	—	—
$\mathbf{I}_e/\mathbf{II}_d$		Cl	168.1[b]	48.2	—	—
$\mathbf{I}_e/\mathbf{II}_e$		Br	170.1[b]	44.2	—	—
$\mathbf{I}_e/\mathbf{II}_f$		CN	171.1	33.1	202.1	21.8
$\mathbf{I}_e/\mathbf{II}_g$		NO_2	171.7	28.5	189.4	21.5
$\mathbf{I}_f/\mathbf{II}_a$	CN	CH_3O	124.1	24.2	202.9	21.8
$\mathbf{I}_f/\mathbf{II}_b$		CH_3	117.8	26.6	167.1	21.0
$\mathbf{I}_f/\mathbf{II}_c$		H	145.1	39.9	177.3	21.2
$\mathbf{I}_f/\mathbf{II}_d$		Cl	142.7	16.8	166.7	21.0
$\mathbf{I}_f/\mathbf{II}_e$		Br	161.4	38.6	180.0	21.3
$\mathbf{I}_f/\mathbf{II}_f$		CN	172.2	18.1	201.1	21.8
$\mathbf{I}_f/\mathbf{II}_g$		NO_2	166.1	14.3	198.1	21.7

[a] Values given are for the 50 mol% compositions.

[b] Direct transition to isotropic.

produce nematogenic complexes with the acid either substituted with the electron-donating (CH_3O and CH_3) or the electron-withdrawing (CN or NO_2) substituents, whereas non-mesomorphic complexes are formed with the unsubstituted or halogen-substituted benzoic acids.

In order to confirm further the formation of a hydrogen-bonded associate between the two non-mesomorphic components, binary phase diagrams were constructed to cover the whole range of composition. Examples are given in Figs. 8 and 9, which represent extremes in the polarity of substituents attached to both sides of the complex. That is, the most electron-donating (CH_3O) and electron-withdrawing (CN) groups were, alternatively, substituted on either side of the complex. As can be seen from Figs. 8 and 9, an enhanced nematic phases are induced in the 1:1 molar mixtures, indicating the formation of hydrogen-bonded complexes. In three of the investigated binary mixtures, namely, $\mathbf{I}_a/\mathbf{II}_a$, $\mathbf{I}_a/\mathbf{II}_f$, and $\mathbf{I}_f/\mathbf{II}_a$, solid hydrogen-bonded complexes are also formed as indicated by the two eutectic points, one preceding and the other following the 1:1 molar composition. It can also be observed from Figs. 8 and 9 that the nematic composition range extends over a wide range of composition, especially when a methoxy group is attached to the pyridine-based component, the proton-acceptor. This is in accordance with the concept of the increased electron density on the pyridine-nitrogen of the proton-acceptor as a result of the electron-donating nature of the methoxy group.

Accordingly, all possible 1:1 molar mixtures, made from each of the six pyridine-based derivatives ($\mathbf{I}_{a-f}$), alternatively, with each of the seven substituted benzoic acids ($\mathbf{II}_{a-g}$), were investigated for their mesophase behavior by DSC and PLM, and the results are collected in Table 3. As can be noted from the table, electron-donating (CH_3O and CH_3), as well as strong electron-withdrawing (CN), groups induce the nematic phase in the resultant associates, independent of the type

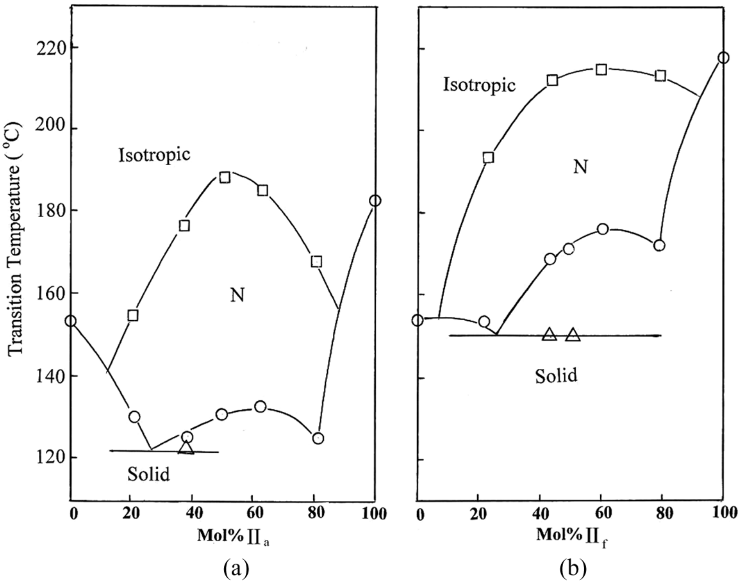

Figure 8. Binary phase diagram of the methoxy-substituted pyridine-based derivative ($\mathbf{I}_a$) with (a) 4-methoxy benzoic acid and (b) 4-cyano benzoic acid.

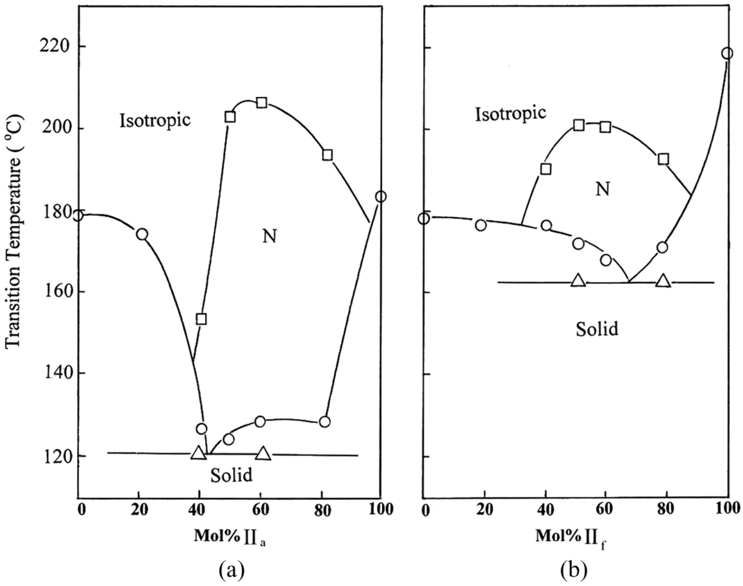

(a) (b)

Figure 9. Binary phase diagram of the cyano-substituted pyridine-based derivative (**I**$_f$) with (a) 4-methoxy benzoic acid and (b) 4-cyano benzoic acid.

of substituent attached to the acid complement. Conversely, the unsubstituted derivative, **I**$_c$, furnishes associates that are non-mesomorphic, independent also of the acid used. The halogen-substituted bases, **I**$_d$ and **I**$_e$, form complexes that are intermediate in behavior. That is, they produce nematogenic (N) associates with the acid substituted either with the electron-donating (CH_3O and CH_3) or electron-withdrawing (CN or NO_2) groups, whereas non-mesomorphic adducts are formed with the unsubstituted or halogen-substituted benzoic acids.

Transition Temperatures and Polarizability Anisotropy of the C$_{ar}$-X and/or C$_{ar}$-Y Bonds

As we concluded above, in hydrogen-bonded liquid crystal complexes, phase behavior is related to the strength of the hydrogen bonds involved [18]. In the pyridine/benzoic acid complexes, the association is primarily affected by the acidity of the proton-donor, the acid, as well as the basicity of the pyridine derivative. The relationship between the stability of the mesophase, expressed as the clearing temperature, T_C, and the anisotropy of polarizability ($\Delta\alpha_X$) of bonds to the small compact terminal substituent (C_{ar}-X), was studied by van der Veen [19]. The relationship has the form:

$$T_C \, \alpha \, (\Delta\alpha_M + \Delta\alpha_X)^2 \tag{1}$$

where T_C is measured in Kelvin. Equation (1) can be put in the form [20]:

$$T_C^{1/2} \, \alpha(\Delta\alpha_M + \Delta\alpha_X) = a \cdot \Delta\alpha_M + a \cdot \Delta\alpha_X \tag{2}$$

The term $\Delta\alpha_M$ is the polarizability anisotropy of all the molecular structure except the terminal substituent, X, and a is the proportionality constant. Thus, if $T_C^{1/2}$ of any of our investigated hydrogen-bonded series bearing one and the same acid substituent **Y** but of varying base substitution **X** is plotted against $\Delta\alpha_X$, a straight line is expected with a slope $a_{(X)}$ and intercept equals to $a_{(X)} \cdot \Delta\alpha_{M(Y)}$, where $a_{(X)}$ is the slope of the $\Delta\alpha_X$-dependency of $T_C^{1/2}$, and $\Delta\alpha_{M(Y)}$ is the polarizability anisotropy of the remainder of the molecular structure except the substituent (**X**) but still including the substituent (**Y**). Figure 10 illustrates the dependency of the $T_C^{1/2}$ values on the polarizability anisotropy of the bonds to X in the pyridine-based component of the supramolecular complex, individually, with the variously substituted acids (**II**$_a$-**II**$_f$).

Alternatively, if $T_C^{1/2}$ values of any series bearing the same pyridine-based substituent (**X**) while the acid components each bears different substituents (**Y**) is plotted

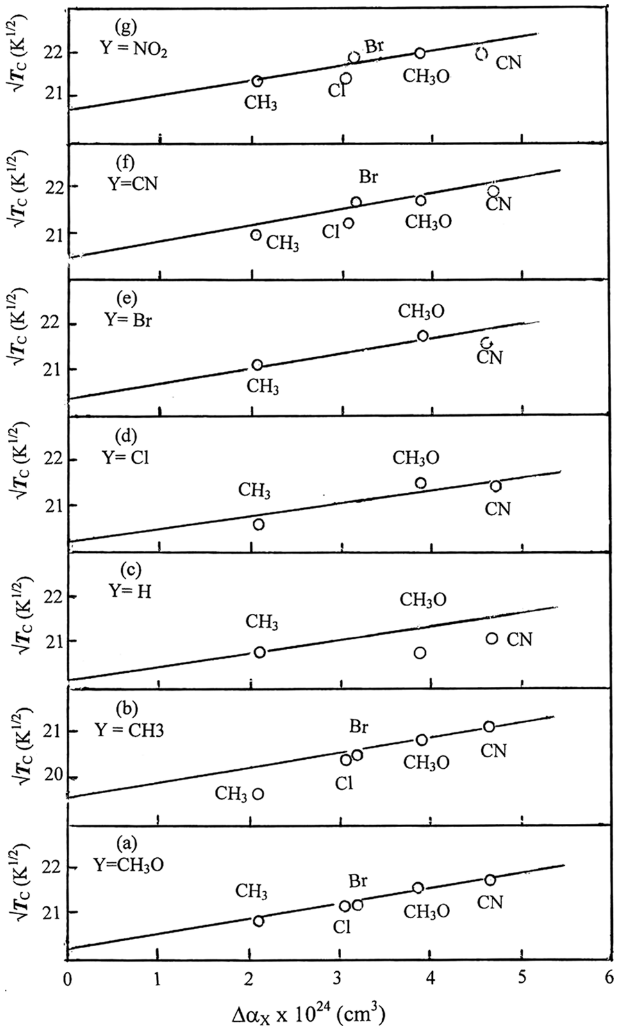

Figure 10. Dependence of the mesophase stability ($T_C^{1/2}$) of the investigated 1:1 adducts of group **B** on the polarizability anisotropy ($\Delta\alpha_Y$) of the pyridine-based substituent (X).

against the polarizability anisotropy ($\Delta\alpha_Y$) of the substituent (**Y**), a straight line is again expected, but in this case the slope is $a_{(Y)}$ and the intercept is $a_{(Y)} \cdot \Delta\alpha_{M(X)}$, where $\Delta\alpha_{M(X)}$ is the polarizability anisotropy of the remainder of the molecular structure comprising the substituent (**X**). The $\boldsymbol{T}_C^{1/2}$ values are again plotted, individually, for each series bearing one and the same substituent **X** as a function of the polarizability anisotropy $\Delta\alpha_Y$ and depicted in Fig. 11. As can be seen from Figs. 10 and 11, fairly linear dependencies were observed in nearly all series investigated. It would be worth mentioning here that the chloro- and bromo-substituted derivatives are more effective than the unsubstituted analogues in stabilizing the hydrogen-bonded complex when added to acids substituted with either electron-donating (CH_3O or CH_3) or electron-withdrawing (CN or NO_2) groups. The electromeric releasing power of the halogen is completely counterbalanced by its electron-withdrawing inductive character, resulting in an increased mesophase stability of the

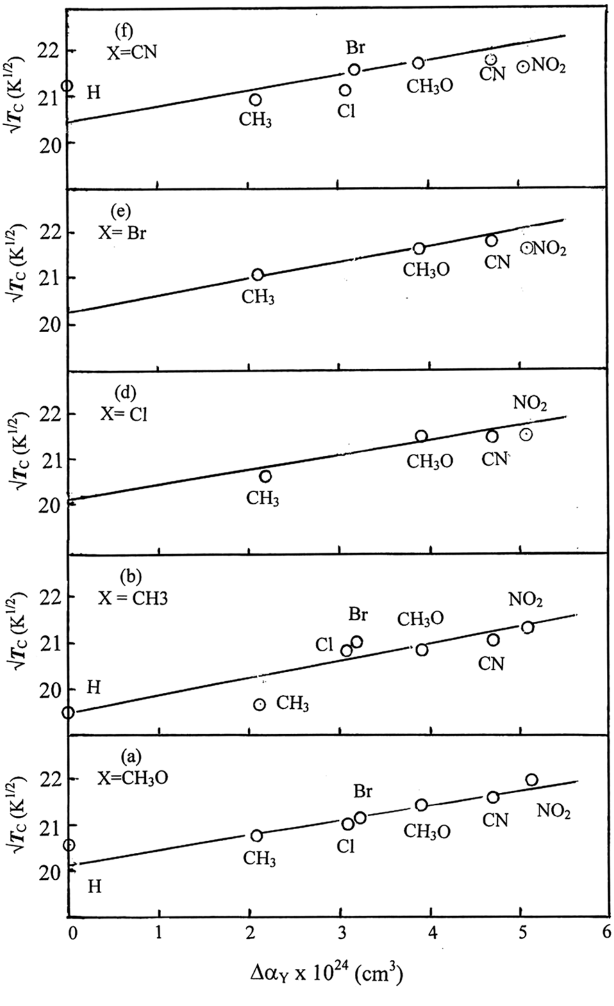

Figure 11. Dependence of the mesophase stability ($\boldsymbol{T}_C^{1/2}$) of the investigated 1:1 adducts of group **B** on the polarizability anisotropy ($\Delta\alpha_X$) of the acid substituent (Y).

Table 4. Regression analyses data for the van der veen correlations for Group **B** complexes

System	X	Y	Slope × 10^{-23}	Intercept	$\Delta\alpha_{M(X)} \times 10^{23}$	$\Delta\alpha_{M(Y)} \times 10^{23}$
I/II$_a$	Varies	CH_3O	3.45	20.17	—	5.85
I/II$_b$	—	CH_3	2.52	19.88	—	7.86
I/II$_c$	—	H	5.75	18.28	—	3.19
I/II$_d$	—	Cl	2.30	19.91	—	8.66
I/II$_e$	—	Br	4.02	19.65	—	4.89
I/II$_f$	—	CN	2.87	20.59	—	7.17
I/II$_g$	—	NO_2	4.02	20.55	—	5.11
I$_a$**/II**	CH_3O	Varies	3.92	19.86	5.07	—
I$_b$**/II**	CH_3	—	3.52	19.60	5.57	—
I$_c$**/II**	H	—	—	—	—	—
I$_d$**/II**	Cl	—	3.49	19.07	5.72	—
I$_e$**/II**	Br	—	4.02	20.25	5.04	—
I$_f$**/II**	CN	—	3.10	20.34	6.56	—

resulting complex as evidenced by their relatively high T_C values (see Table 3, where **X** = Cl or Br while **Y** is CN, NO_2, CH_3O, or CH_3).

Figures 10 and 11 were used to calculate the slope and intercept of each of their regression lines from which $\Delta\alpha_{M(X)}$ and $\Delta\alpha_{M(Y)}$ are calculated. Results of the computation, as given in Table 4, show that the polarizability anisotropy $\Delta\alpha_{M(Y)}$ of the complex, except substituent **X,** decreases according to **Y** in the order:

$$Cl > CH_3 > CN > CH_3O > NO_2 > Br > H.$$

The high anisotropy of polarizability of the nitro-substituted complex may be ascribed to the high molecular ordering observed in the pure solid component ($\Delta S = 28.3/(179.3 + 273) = 62.5$ J/mol/K).

On the other hand, as can also be deduced from Table 4, the polarizability anisotropy, $\Delta\alpha_{M(X)}$, of the complex, except substituent **Y**, decreases according to **X** in the order:

$$CN > Cl > CH_3 > CH_3O > Br > H.$$

Table 5. Regression analyses data for the van der veen correlations for Group **A** complexes

System	n	Slope × 10^{-23}	Intercept	$\Delta\alpha_M \times 10^{23}$
I/II8	8	2.02	20.07	9.94
I/II10	10	3.11	19.44	6.25
I/II12	12	3.47	19.40	5.59
I/II14	14	2.26	19.57	8.66
I/II16	16	1.06	20.20	19.06

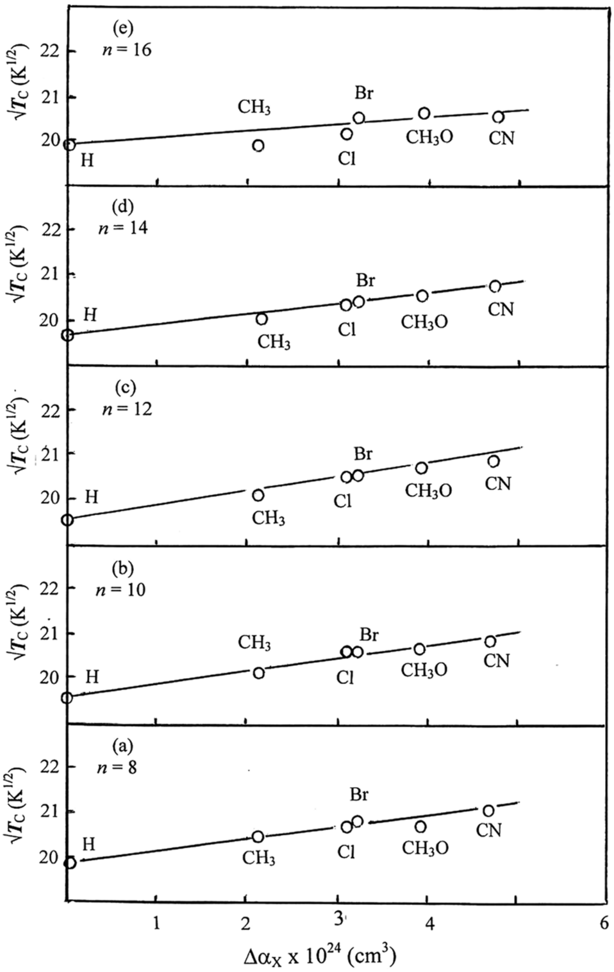

Figure 12. Dependence of the mesophase stability ($T_C^{1/2}$) of the investigated 1:1 adducts of group **A** on the polarizability anisotropy ($\Delta\alpha_X$) of the pyridine-based substituent (X).

This order again revealed the priority of the halogen substituents over hydrogen, either on the acid side or on the pyridine-based components in promoting the mesophase.

Similar dependencies were made for group **A** complexes (Table 5). Thus, $\sqrt{T_C}$ is plotted in Fig. 12 against $\Delta\alpha_X$ of substituents X on the pyridine-based derivative. Linear correlations are again obtained.

Conclusions

Six laterally methyl-substituted pyridine-based azo dye derivatives of the type 4-(4′-pyridylazo-3-methyl phenyl)-4″-substituted benzoates, $\mathbf{I}_{a-f}$, were prepared in which the terminal substituent varies between CH_3O, CH_3, H, Cl, Br, and CN groups, respectively. The CH_3 group was laterally introduced into the central benzene ring in order to modify their melting temperatures. The effect of polarity of the terminal substituent on the possibility of formation, and the stability of the mesophase of the resulting adducts was investigated via differential scanning calorimetry and polarized optical microscopy. Two groups of hydrogen-bonded supramolecular complexes were prepared and investigated for their mesophase behaviors. In the first, group **A**, five homologues of the 4-alkoxybenzoic acids were used and the 1:1 molar complex formation was confirmed by constructing their corresponding binary phase diagrams with two representative homologues of the acid. In the second group of complexes (group **B**), the acid complements, $\mathbf{II}_{a-g}$, were substituted alternatively with seven substituents of different polarity, namely, CH_3O, CH_3, H, Cl, Br, CN, and NO_2, respectively. The study revealed the following:

1. As evidenced from their binary-phase diagrams, except for the unsubstituted derivative, $\mathbf{I}_c$, that showed only the SmC mesophase, with all homologues of the acids investigated, mixtures in their 1:1 molar ratio proved to exhibit SmC mesophase.
2. Again, except for the unsubstituted derivative, $\mathbf{I}_c$, other analogues proved to form supramolecular hydrogen-bonded complexes with all the investigated homologues of the acids, as evidenced from their enhanced mesophase stability at the 1:1 molar ratio.
3. With respect to group **B** complexes, both electron-donating (CH_3O and CH_3) and electron-withdrawing (NO_2 and CN) on either end of the complexes have shown to induce a nematic phase in the 1:1 molar mixtures of the two non-mesomorphic components ($\mathbf{I}_{a-f}$ and $\mathbf{II}_{a-g}$). Conversely, the complexes of the unsubstituted derivative, $\mathbf{I}_c$, showed no mesophases with either of the substituted acids. Those with the intermediate polarity, *i.e.*, the Cl- and Br-substituted analogues showed the nematic mesophase only when complexed with benzoic acids substituted with strong polar groups, namely, CH_3O, CH_3, CN, and NO_2.
4. Comparison between the present results and those previously reported [12] for the laterally neat derivatives ($\mathbf{III}_{a-e}$) revealed that methyl-lateral substitution into the central benzene ring of the pyridine-based compounds resulted in a lowering of melting point but significantly affected the mesophase behavior of their hydrogen-bonded complexes with substituted benzoic acids.
5. The stability of the mesophase, expressed as the clearing temperature, is found to be greatly influenced by the nature of the substituent on either side of the new elongated mesogen.
6. Acceptable linear correlations of $\sqrt{T_C}$ with the polarizability anisotropy of bonds to substituent attached to either end were obtained.

References

[1] Naoum, M. M., Saad, G. R., Nessim, R. I., Abdel Aziz, T. A., & Seliger, H. (1997). *Liq. Cryst.*, *23*, 789.

[2] Nessim, R. I., Naoum, M. M., Mohamed, S. Z., & Nessim, M. I. (2004). *Liq. Cryst.*, *31*, 649.

[3] Vora, R. A., & Prajapati, A. K. (1999). *Liq. Cryst.*, *25*, 567.

[4] Prajapati, A. K. (2000). *Liq. Cryst.*, *27*, 1017.

[5] Prajapati, A. K. (2000). *Mol. Cryst. Liq. Cryst.*, *348*, 65.

[6] Prajapati, A. K., & Pandaya, H. M. (2003). *Mol. Cryst. Liq. Cryst.*, *393*, 31.

[7] Kaspar, M., Bubanov, A., Hamplova, V., & Glogorova, S. P. (2000). *Liq. Cryst.*, *31*, 821.

[8] Mohammady, S. Z., Nessim, R. I., Shehab, O. R., & Naoum, M. M. (2005). *Liq. Cryst.*, *32*, 477.

[9] Lehn, J. M. (1988). *Angew. Chem. Int. Ed. Engl.*, *27*, 89.
[10] Constantinos, M. P., & Dimitris, T. (2001). *Liq. Cryst.*, *28*, 1127.
[11] Price, D. J., Adams, H., & Bruce, D. W. (1999). *Mol. Cryst. Liq. Cryst.*, *289*, 127.
[12] Naoum, M. M., Fahmi, A. A., & Alaasar, M. A. (2008). *Mol. Cryst. Liq. Cryst.*, *482*, 57.
[13] Naoum, M. M., Fahmi, A. A., & Alaasar, M. A. (2008). *Mol. Cryst. Liq. Cryst.*, *487*, 74.
[14] Naoum, M. M., Fahmi, A. A., & Alaasar, M. A. (2009). *Mol.Cryst. Liq. Cryst.*, *506*, 22.
[15] Song, X., Li, J., & Zhang, S. (2003). *Liq. Cryst.*, *30*, 331.
[16] Cammenga, H. K., Eysel, W., Gmelin, E., Hemmiger, W., Hoehne, G. W. H., & Sagre, S. M. (1993). *Thermochim. Acta*, *219*, 333.
[17] Bernhardt, H., Weissflog, W., & Kresse, H. (1996). *Angew. Chem. Int. Ed. Engl.*, *35*, 874.
[18] Paleos, C. M., & Tsiourvas, D. (2001). *Liq. Cryst.*, *28*, 1128.
[19] van der Veen, J. (1975). *J. Phys. Colloq. C1*, *36*, 375.
[20] Naoum, M. M., Saad, G. R., Nessim, R. I., & Abdel Aziz, T. A. (1998). *Liq. Cryst.*, *25*, 73.